ELSEVIER

Chemical Engineering Journal 65 (1997) 133–143

Chemical Engineering Journal

A generalized approach for dynamic modelling and simulation of biofilters: application to waste-water denitrification

Jérôme Jacob [a], Jean-Marc Le Lann [a,*], Hervé Pingaud [a], Bernard Capdeville [b]

[a] *LEAP/AFP: Groupe d'Analyse Fonctionnelle des Procédés, INPT/ENSIGC, 18 Chemin de la loge, 31078 Toulouse Cedex, France*

[b] *INSAT/URTB: Unité de Recherche Traitement Biologique, Complexe scientifique de Rangueil, 31077 Toulouse Cedex, France*

Received 23 September 1996; accepted 15 November 1996

Abstract

This contribution is devoted to the use of dynamic simulation as a support tool to improve the knowledge of biofilters in the general context of waste-water treatment.

After a brief overview of current waste-water treatment techniques, a general approach for modelling and simulation of biofilters in transient states is presented. First of all, a comprehensive description of the development of the model, highlighting specific characteristics such as the active/deactivated biomass approach is presented; discussion of the different phenomena involved is then pursued. The resulting set of Partial Differential Algebraic Equations (PDAE), with the need for state event detection for filter clogging, is then solved using an extension of the Differential–Algebraic philosophy coupled with the method of lines.

Finally, the validity of the general developed model, as well as the reliability of the numerical approach is illustrated through different case studies for denitrification purposes, with plant data comparison.

It demonstrates the utility of dynamic simulation to speed up the development of the model phase and to improve basic knowledge in a new emerging area. © 1997 Elsevier Science S.A.

Keywords: Dynamic simulation and modelling; Wastewater treatment; Denitrification; Biofilters; Partial differential algebraic equations (PDAE)

1. Introduction

Waste-water treatment (and, more generally, environment protection) is a topic that is currently receiving substantial public attention. It consists of a complex sequence of interdependent biological, physical and chemical processes subject to time-varying hydraulic and organic load conditions.

In this context, dynamic simulation based on rigorous mathematical models is a powerful tool by which the designers of new biological waste-water treatment units can investigate the performance of complex systems under different conditions. The use of general dynamic models can assist in improving both basic knowledge at the outset and future operability. Also it may help to develop control strategies, start-up and shutdown procedures and operator training in the wider context of operational water-quality management.

The literature clearly shows that pressure of different regulatory acts (strict limits on BOD, COD and nitrogen discharges) and the complexity of waste-water plants have provided incentives to use process simulation methodology [1]. Among the different case studies reported, it may be noticed that most are devoted to the simulation of activated-sludge waste-water treatment plants [2–5] whereas few contributions in the literature have involved biofilters [6]. However, even in the field of activated-sludge processes, most of the specialists are convinced that model improvement, model evaluation and better calibration are necessary as well as improvements in mathematical tools and techniques, especially for process operation and full-scale dynamics applications. As proof of this situation, a recent motivation at European level has been stimulated by the COST 682 project entitled: 'Optimizing the design and operation of biological waste-water treatment plants through the use of computer programs based on dynamic modelling of the process'.

This paper reports the systematic use of a model based on dynamic simulation for water plant involving submerged biofilters. This class of unit operations is often used for denitrification, nitrification and carbon removal (Biocarbon process, Biofor process...). The main advantages are compactness and the high capacity for removal of carbon, nitrogen and phosphorus. Furthermore, they are well integrated into the environment (no noise, no smell and no aerosols), there

* Corresponding author.

PII S1385-8947(96)03185-3

is no need for secondary clarification except for certain aerobic applications, there is no need for liquid circulation for nitrogen removal, and energy consumption along with sludge production are minimum. One of the main difficulties, from an operational point of view, is due to the cyclic mode of operation and in bed clogging which needs to be anticipated. With these objectives in mind, the proposed generalized model has been developed for submerged biofilters.

2. Modelling of the biofilter

2.1. Basis for biofilter modelling

A biological filter may be described as a three-phase packed column. The solid phase consists of two components: carrier particles (packing) and biofilm (biomass) consisting of water, microorganisms and saccharidic polymers. The gaseous phase consists of air (for aerobic reactions) and products of the reaction (carbon dioxide and, in the case of denitrification, gaseous nitrogen).

Generally, two main parts can be distinguished in a model of a packed biofilter: • a reactor model (hydrodynamic aspect); and • a biofilm model with substrate uptake, product formation and biomass development.

In our particular case, another part has to be added for deep filtration as the suspended particles present in the waste water (and their retention in the filter) are taken into account.

For hydrodynamic aspects, the gaseous phase is not taken into account because the gaseous hold-up is markedly lower than the liquid hold-up.

The biofilter should, rigorously, be described as a series of completely mixed tanks or as a plug-flow reactor with axial dispersion model [7]. Experimental hydrodynamic studies on a biological filter showed that the axial dispersion may be neglected especially for anaerobic reactions: the filter was described by a series of 16 to 60 (for anaerobic treatment) and 11 to 34 (for aerobic treatment) completely mixed tanks. This number, which depends on the experimental conditions (aerobic or anaerobic reactions, air/water flow-rate ratio, degree of clogging of the filter...), is fairly high and we may consider, like most authors [6,8], that the liquid is in plug-flow.

In most biofilter models, stationary and uniform flow is hypothesized. This hypothesis, which simplifies the equations and leads, sometimes, to analytical solutions, may be applied only to very short treatment times. For longer treatment times (as in waste-water treatment), there is progressive clogging of the filter due to biomass growth and retention of suspended particles; it is taken into account in the model by writing a space balance which expresses the progressive diminution of the porosity (volume fraction for the liquid).

For biofilm modelling, four steps are generally considered: • diffusion of substrates through the liquid film layer around the biofilm to the liquid/biofilm interface; • diffusion of substrates through the biofilm; • biological reaction; and • biofilm detachment (which is not taken into account in the model because it is not observed experimentally—the liquid flow is laminar).

In most biofilter models [8,9], diffusion phenomena are taken into account and described by Fick's law. From a theoretical point of view, the diffusion is a phenomenon which occurs perpendicularly to the liquid flow through a flat surface. In biological filtration, the biofilms are very irregular and filamentous which accords poorly with the diffusional theory hypothesis.

Furthermore, experimental studies on aerobic [10] and anaerobic [11] biofilms show that the substrate removal reaction occurs only at the edge of the biofilm in a very thin part of it—the active thickness is estimated at about 10 μm whereas the biofilm may reach 500 μm. Thus, the reaction may be considered as a surface reaction.

Fig. 1 shows the evolution of the amount of biomass (active and total) and the biofilm aspect (front and profile

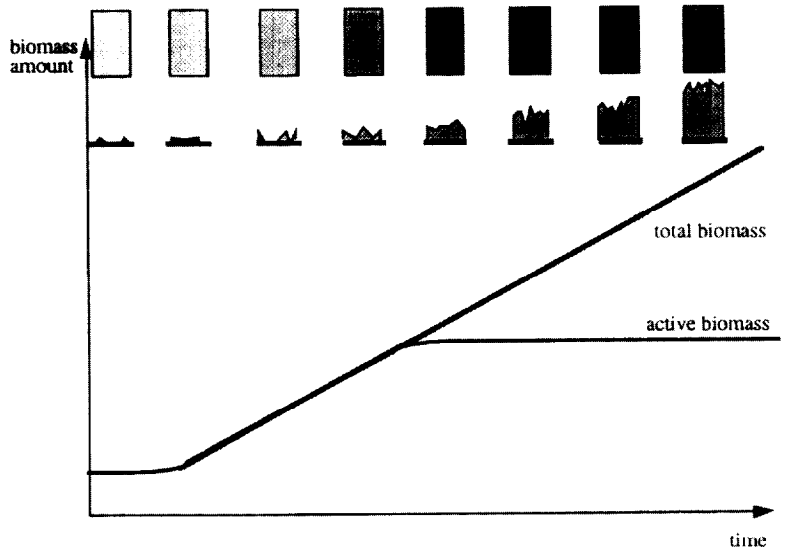

Fig. 1. Total and active biomass evolution.

views) with time. At the beginning, the active biomass grows at the edge of the particles. Then, when the support is fully settled by microorganisms, the active biomass becomes constant while the total biomass keeps on growing; when reaction occurs the microorganisms grow at the edge of the biofilm and a new active layer is generated which deactivates the previous one.

For these reasons, diffusion phenomena, as in some other works [6,12], are not taken into account in the model.

2.2. *Model of the biological reaction*

Initially, a model is built considering the whole biomass active in the filter. This approach is based on a contradiction but it is interesting to try it in order to emphasize the falseness of the hypothesis it is based on.

The biological model is adapted from the general model of the IAWPRC for activated sludge process [5]; in this first approach, microorganism growth is first-order with total biomass (concentration X_B) with double substrate limitation characterized by a double Monod-type kinetic law for the electron donor D and the electron acceptor A. The general form is:

$$\frac{\partial X_B}{\partial t} = \mu_{max}\left(\frac{S_D}{S_D + K_D}\right)\left(\frac{S_A}{S_A + K_A}\right)X_B$$

and it may be applied to every kind of reaction which might occur in a biofilter (Table 1).

As in the first IAWPRC model, the stoichiometric coefficients are obtained by writing reduction-degree balances for the biological reaction. For example, in denitrification:

$$\frac{1}{Y_H}\text{ organic substrate} + \frac{1 - Y_H}{2.86 Y_H}\text{ nitrate} \rightarrow \text{ biomass}$$

where Y_H is the heterotrophic biomass yield.

For $1/Y_H$ mol (COD) of electrons given by the organic substrate, 1 mole (COD) of biomass is formed, the nitrates using the rest are completely reduced to gaseous nitrogen.

The organic compound concentrations are given in units of chemical oxygen demand (COD), likewise the balances are written in terms of COD, and hence a conversion term (here 2.86) is used to transform to COD the nitrogen compound concentrations (given as nitrogen).

In the IAWPRC model for activated sludge, the decay of the microorganisms is taken into account (as hydrolysis and ammonification) because, in these types of process, the biomass is not fixed and the solid residence time is long (approximately 3–15 days). The biofilter, on the other hand, has to be washed frequently to prevent clogging, that induces short solid residence time (approximately 1–3 days) and the biomass decay may be neglected. Likewise, after experimental observation, it has been decided to neglect biofilm detachment during the treatment phase.

As the first approach is based on a contradiction (we consider the whole biomass active although it has been shown that only microorganisms present at the edge of the biofilm are working in the biological reaction), we use a more realistic approach based on the concept of active/deactivated biomass (M_a/M_d). The principle is described below [10,11].

- The active microorganisms are responsible for substrate degradation and are characterized by a specific growth rate μ_0:

$$\mu_0 = \mu_{max}\left(\frac{S_D}{S_D + K_D}\right)\left(\frac{S_A}{S_A + K_A}\right)$$

- The deactivated microorganisms do not play any role in substrate degradation (even though they might maintain their enzymic activity) but continue to play a role in filter clogging.
- The total biomass is defined as the sum of the two types of biomass $X_B = X_A + X_D$.

An intrinsic kinetic (without considering deactivation of the active biomass) is defined:

$$\left(\frac{\partial X_A}{\partial t}\right)_i = r_a = \mu_0 X_A$$

As shown in Fig. 1, when the support is fully populated by microorganisms, part of the active biomass (at the edge of the biofilm) keeps on growing while another part has lost its activity, which induces an accumulation of deactivated biomass:

Table 1
Kinetics for the different applications of biofiltration

Reaction	Characteristics	Kinetics
Denitrification Reduction of nitrates to gaseous nitrogen	Anaerobic work of heterotrophic biomass Electron donor: organic substrate Electron acceptor: nitrates	$\frac{\partial X_B}{\partial t} = \eta_g \mu_H \left(\frac{S_S}{S_S + K_S}\right)\left(\frac{S_{NO_3}}{S_{NO_3} + K_{NO_3}}\right)X_B$
Denitritation Reduction of nitrites to gaseous nitrogen	Anaerobic work of heterotrophic biomass Electron donor: organic substrate Electron acceptor: nitrites	$\frac{\partial X_B}{\partial t} = \eta_g \mu_H \left(\frac{S_S}{S_S + K_S}\right)\left(\frac{S_{NO_2}}{S_{NO_2} + K_{NO_2}}\right)X_B$
Nitrification Oxidation of ammonia to nitrates	Aerobic work of autotrophic biomass Electron donor: ammonia Electron acceptor: oxygen	$\frac{\partial X_B}{\partial t} = \mu_A \left(\frac{S_{NH}}{S_{NH} + K_{NH}}\right)\left(\frac{S_O}{S_O + K_{OA}}\right)X_B$
Carbon removal Oxidation of organic substrate	Aerobic work of heterotrophic biomass Electron donor: organic substrate Electron acceptor: oxygen	$\frac{\partial X_B}{\partial t} = \mu_H \left(\frac{S_S}{S_S + K_S}\right)\left(\frac{S_O}{S_O + K_{OH}}\right)X_B$

$$\left(\frac{\partial X_A}{\partial t}\right)_d = r_d = K_1 I X_A$$

where I is the concentration of inhibiting products, proportional to the active amount of biomass

$$I = \alpha X_A \Rightarrow r_d = K_1 \alpha X_A^2 = K_2 X_A^2$$

So, the real active biomass accumulation is:

$$\left(\frac{\partial X_A}{\partial t}\right)_{acc} = \left(\frac{\partial X_A}{\partial t}\right)_i - \left(\frac{\partial X_A}{\partial t}\right)_d = r_a - r_d = \mu_0 X_A - K_2 X_A^2$$

When the 'steady state' is reached:

$$\left(\frac{\partial X_A}{\partial t}\right)_{acc} = 0 \text{ and } X_A = X_{Amax} \Rightarrow K_2 = \frac{\mu_0}{X_{Amax}}$$

Thus, the real growth kinetics for the active and total biomass are:

$$\frac{\partial X_A}{\partial t} = \mu_0 X_A \left(1 - \frac{X_A}{X_{Amax}}\right)$$

$$= \mu_{max}\left(\frac{S_D}{S_D + K_D}\right)\left(\frac{S_A}{S_A + K_A}\right) X_A \left(1 - \frac{X_A}{X_{Amax}}\right)$$

$$\frac{\partial X_B}{\partial t} = \frac{\partial X_A}{\partial t} + \frac{\partial X_D}{\partial t} = \mu_0 X_A = \mu_{max}\left(\frac{S_D}{S_D + K_D}\right)\left(\frac{S_A}{S_A + K_A}\right) X_A$$

2.3. Model for the physical reaction (deep filtration)

Unlike other biofilter models, we take into account the suspended particles in the influent and their retention in the filter. Two types of deep filtration models exist:

- macroscopic models with material balances and a kinetic equation introducing a hold-up probability [13]; and
- microscopic models which describe the biofilter as an aggregation of single collectors with specific geometry, introducing the suspended-particle diameter [14].

A granulometric analysis of the waste water shows a range of particle size (with two sensible peaks around 10 μm and 50 μm); thus, it seems better to use the macroscopic approach.

The physical filtration reaction may be written:suspended particles (M_l) → retained particles (M_r)

The retention kinetic is:

$$\frac{\partial X_{M_r}}{\partial t} = \frac{Q k X_{M_l}}{\Omega}$$

where k is the filtration coefficient, corresponding to the probability density of particle capture.

To a first approximation, this coefficient may be considered as a constant; this is the choice used in the model. But, in fact, it is logical to think that the filtration efficiency decreases as soon as the retention sites are occupied by the captured particles.

The filtration coefficient is defined as a function of the retention in the filter (volume fraction occupied by captured particles) [15];

$$k = k_0 F(\sigma)$$

Different forms of the function $F(\sigma)$ were tried ($F(\sigma) = 1 - \sigma/\sigma_M$, $F(\sigma) = 1 - (\sigma/\sigma_M)^2$, where σ_M is the maximum retention when all the sites are occupied and the retention probability is equal to zero) but as none gave significant results, we kept the first option.

2.4. Resulting set of equations for the model

A material balance is written for each component on an elementary volume, for a liquid in plug flow inside the filter:accumulation = input − output ± reaction

$$\frac{\partial [\,] dV}{\partial t} = Q([\,]_z - [\,]_{z+dz}) + \nu r dV$$

where ν is the stoichiometric coefficient for the component involved in reaction r.

These material balances are combined with the space balance—the variations of the void fraction (or porosity ϵ) are due to the growth of total biomass and the retention of suspended particles:

$$\frac{\partial \epsilon}{\partial t} = -\left(\frac{1}{d_{cell}}\frac{\partial X_B}{\partial t} + \frac{1}{d_{part}}\frac{\partial X_{M_r}}{\partial t}\right)$$

2.4.1. Basic assumptions of the model

- The liquid is in plug flow.
- The liquid flow-rate is supposed to be constant inside the filter but variations in feed flow-rate are taken into account.
- Suspended particles in the influent are taken into account.
- Filter clogging is taken into account.
- Diffusion phenomena are not taken into account.
- The gaseous phase is not taken into account.
- The initial amount of biomass is uniform in the filter.
- Decay of biomass is neglected.
- Detachment of biofilm and retained particles is neglected (laminar flow).
- Temperature and pH (close to 7) are constant in the filter.

For the M_a/M_d approach, a system of eight partial differential equations, with adequate initial and boundary conditions, is obtained (Table 2). For floating bed biofilters, an algebraic equation may be added to represent the bed rising in the filter. For aerobic reactions (carbon removal, nitrification), a term for oxygen transfer in the liquid phase, $k_L a (S_o^* - S_o)$, has to be added in the oxygen material balance (S_o^* is the concentration in equilibrium with the gaseous phase, the maximum solubility of oxygen in the water, $k_L a$ is the transfer coefficient of the oxygen in the liquid).

The pressure drop in the filter is calculated by means of the Blake–Kozeny correlation [16]:

$$\Delta P = \Delta z \frac{150 \mu U_m (1-\epsilon)^2}{D_p^2 \epsilon^3}$$

where μ is the dynamic viscosity, D_p the particle diameter and U_m the superficial velocity of the liquid.

If the reactor is divided into n elementary volumes of height Δz, the total pressure drop is:

Table 2
System of equations for Ma/Md approach

Component	Balance	Initial and boundary conditions
Total biomass	$\frac{\partial X_B}{\partial t}=\mu_{max}\left(\frac{S_D}{S_D+K_D}\right)\left(\frac{S_A}{S_A+K_A}\right)X_A$	$X_B(t=0)=X_{A0}$
Active biomass	$\frac{\partial X_A}{\partial t}=\mu_{max}\left(\frac{S_D}{S_D+K_D}\right)\left(\frac{S_A}{S_A+K_A}\right)X_A\left(1-\frac{X_A}{X_{Amax}}\right)$	$X_A(t=0)=X_{A0}$
Retained particles	$\frac{\partial X_{M_r}}{\partial t}=\frac{QkX_{M_1}}{\Omega}$	$X_{M_r}(t=0)=0$
Electron donor	$\frac{\partial(\epsilon S_D)}{\partial t}=-\frac{Q}{\Omega}\frac{\partial S_D}{\partial z}-\nu_D\mu_{max}\left(\frac{S_D}{S_D+K_D}\right)\left(\frac{S_A}{S_A+K_A}\right)X_A$	$S_D(t=0)=S_D(z=0)=S_{D(input)}$
Electron acceptor	$\frac{\partial(\epsilon S_A)}{\partial t}=-\frac{Q}{\Omega}\frac{\partial S_A}{\partial z}-\nu_A\mu_{max}\left(\frac{S_D}{S_D+K_D}\right)\left(\frac{S_A}{S_A+K_A}\right)X_A$	$S_A(t=0)=S_A(z=0)=S_{A(input)}$
Ammonia (or nitrates in case of denitrification)	$\frac{\partial(\epsilon S_N)}{\partial t}=-\frac{Q}{\Omega}\frac{\partial S_N}{\partial z}-\nu_N\mu_{max}\left(\frac{S_D}{S_D+K_D}\right)\left(\frac{S_A}{S_A+K_A}\right)X_A$	$S_N(t=0)=S_N(z=0)=S_{N(input)}$
Suspended particles	$\frac{\partial(\epsilon X_{M_1})}{\partial t}=-\frac{Q}{\Omega}\frac{\partial X_{M_1}}{\partial z}-\frac{QkX_{M_1}}{\Omega}$	$X_{M_1}(t=0)=X_{M_1}(z=0)=X_{M_{1(input)}}$
Porosity	$\frac{\partial\epsilon}{\partial t}=-\frac{\mu_{max}}{d_{cell}}\left(\frac{S_D}{S_D+K_D}\right)\left(\frac{S_A}{S_A+K_A}\right)X_A-\frac{QkX_{M_1}}{d_{part}\Omega}$	$\epsilon(t=0)=\epsilon_0$

$$\Delta P_T=\sum_{i=1}^{n}\Delta P_i$$

3. Numerical method and implementation aspects

The equations describing filter behaviour lead to a partial differential algebraic system (PDAE) which may be written in vectorial form with adequate initial and boundary conditions:

$$\boldsymbol{D}(s,t)\frac{\partial \boldsymbol{s}}{\partial t}=\boldsymbol{f}(\boldsymbol{s},t,\boldsymbol{u},\boldsymbol{p})+\boldsymbol{g}(\boldsymbol{s},t,\boldsymbol{u},\boldsymbol{p})\frac{\partial \boldsymbol{s}}{\partial z} \quad (1)$$

$$\boldsymbol{s}(t=0)=\boldsymbol{s}_0,\ z \quad \boldsymbol{s}(z=0)=\boldsymbol{s}_{input},\ t$$

where $\boldsymbol{s}$ is the vector of the state variables, $\boldsymbol{u}$ the vector of the control variables and $\boldsymbol{p}$ the vector of the input variables.

Different numerical methods (orthogonal collocation, method of lines...) may be used to solve this kind of system. Bearing in mind generalization, a numerical strategy issued from the solving of mixed differential and algebraic equations system (DAE), coupled with the method of lines with fixed-grid discretization has been implemented.

The numerical method of lines (NMOL) [17] may be considered as one of the most powerful tools for the solution of time-dependent coupled ODE/PDE systems. The attraction of this method is that the complex system of coupled ordinary and partial differential equations arising in mathematical modelling can be solved by using the sophisticated tools which have been developed for initial value differential–algebraic equations. Additionally, the proposed extended DAE approach to PDAE allows global resolution with no discrimination between the variables of the system as it is given by the model designer and the use of robust and reliable implicit numerical integrators.

The principle of the method of lines is to discretize the spatial variable (z) into $n-1$ pieces (n is the discretization order). Each variable is transformed into n variables corresponding to its value at each of the n positions in the filter. The spatial derivatives are approximated using finite differences. After preliminary numerical studies, an approximation formula with five points has been chosen. The general term is

$$\frac{\partial s_i}{\partial z}=\frac{2s_{i-2}-16s_{i-1}+16s_{i+1}-2s_{i+2}}{\Delta z.4!} \quad i=3 \text{ to } i=n-2$$

while special formulae are used for the upper and lower boundaries:

$$\frac{\partial s_1}{\partial z}=\frac{-50s_1+96s_2-72s_3+32s_4-6s_5}{\Delta z.4!}$$

$$\frac{\partial s_2}{\partial z}=\frac{-6s_1-20s_2+36s_3-12s_4+2s_5}{\Delta z.4!}$$

$$\frac{\partial s_{n-1}}{\partial z}=\frac{-2s_{n-4}+12s_{n-3}-36s_{n-2}+20s_{n-1}+6s_n}{\Delta z.3!}$$

$$\frac{\partial s_n}{\partial z}=\frac{6s_{n-4}-32s_{n-3}+72s_{n-2}-96s_{n-1}+50s_n}{\Delta z.4!}$$

Thus, the system is transformed into a system of $8n$ ordinary (or algebraic) differential equations which are solved by Gear's multistep multi-order implicit method based on a predictor corrector scheme [18–20].

At any time step, a set of variables is computed using extrapolation polynomials based on the values of the variables and their derivatives at previous steps (prediction phase). The number of previous steps used is the order of the method. The correction phase consists in correcting the predicted values to reach the solution, by using an approximation of the derivative

$$\frac{\partial s}{\partial t} = \frac{1}{h\beta}(s - \psi)$$

where h is the time step, β a parameter depending of the order and ψ a function of the variable values at previous steps. Thus, the system described by Eq. (1) becomes a non-linear algebraic equations system:

$$\boldsymbol{g}(\boldsymbol{s}, t, \boldsymbol{u}, \boldsymbol{p}) = h\beta \boldsymbol{f}(\boldsymbol{s}, t, \boldsymbol{u}, \boldsymbol{p}) - \boldsymbol{D}(\boldsymbol{s}, t)(\boldsymbol{s} - \psi) = 0$$

This is then solved by a Newton–Raphson method. The values used for the initialization came from the prediction phase:

$$\boldsymbol{s}^{k+1} = \boldsymbol{s}^k + \delta \boldsymbol{s}^k$$

where δs^k is the solution of the linear system:

$$\left[h\beta \boldsymbol{J}^k - \frac{\partial \boldsymbol{D}^k}{\partial \boldsymbol{s}^k}(\boldsymbol{s}^k - \psi) - \boldsymbol{D}^k \right] \delta \boldsymbol{s}^k = -\boldsymbol{g}(\boldsymbol{s}^k, t, \boldsymbol{u}^k, \boldsymbol{p})$$

where $\boldsymbol{J}^k$ is the jacobian matrix of the elements $\partial f_i / \partial s_j$.

This system may be written

$$\boldsymbol{M}^k \delta \boldsymbol{s}^k = -\boldsymbol{g}(\boldsymbol{s}^k, t)$$

where $\boldsymbol{M}^k$, called the dynamic operator, is the dynamic equivalent of the jacobian matrix in steady-state.

When the corrector converges, numerical tests are performed to validate the integration step with a tolerance given by the user. These tests activate a step and order change strategy to provide a good result quality for a lower cost.

As seen previously, at any time step a non-linear system in the corrector loop has to be solved. For a rapid convergence and because there is a good initialization with the predictor, the Newton–Raphson method is chosen, involving analytical derivatives in the dynamic operator.

The eight equations of the model are arranged for each discretization point which leads to a block structure for the dynamic operator (Fig. 2). Each block is an 8×8 matrix corresponding to the model equation at one discretization point. These equations are arranged to bring the non-zero terms closer to the diagonal and to preferably fill the upper triangular part of the block. The extra diagonal blocks come from the spatial five-point derivative approximation. The operator, partially hollow, is an n-diagonal block matrix and computation time, reliability and efficiency is gained by treating it like a banded matrix: it is transformed in a smaller rectangular matrix for which the pivot research in the Gaussian elimination is done vertically.

As the biofilter has a cyclic operating mode and is cleaned when the pressure drop reaches an upper limit ($\Delta P = \Delta P_{max}$), an automatic procedure to detect state events has been implemented [21]. In the case of time events, input disturbance discontinuities are represented by using a polynomial approximation to simulate step or ramp functions.

The numerical strategy has appeared to be very efficient and reliable. The main interest in the method of lines leads to the fact that all the development involved in DAE systems may be re-used. One of its drawbacks is in the discretization scheme which is a fixed-grid approach and may be overcome by applying a variable grid strategy. However, in our case, this was not a necessity as there were no sharp space profiles.

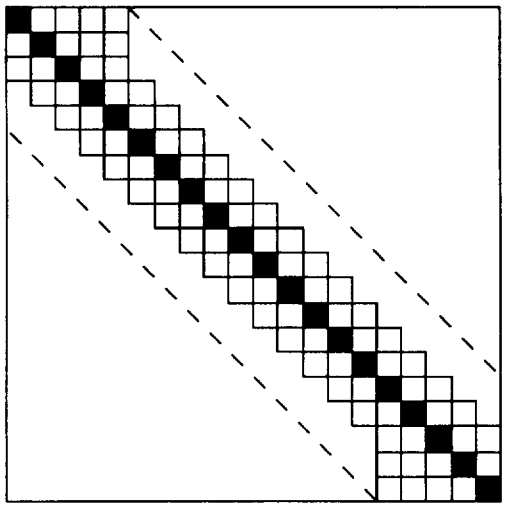

Fig. 2. The dynamic operator.

4. Experimental and dynamic simulation studies

4.1. Pilot plant description

Even if the type of applications (denitrification, denitritation, waste water, drinking water...) and operational conditions (up-flow, down-flow...) used are different, all of the experiments presented in this paper were performed with the same pilot biofilter, which was designed and performed as a multipurpose flexible biofilter.

The biofilter diameter was 6.8 cm and packed height 2.1 m; sample points were placed every 30 cm and it was packed with pouzzolane (a very porous volcanic rock). The reactor configuration is presented for the case of denitrification of a drinking water (up-flow for a synthetic water using ethanol as the organic carbon source) in Fig. 3.

Table 3 gives the values of kinetic, stoichiometric and filtration parameters used in the following applications.

4.2. Application to the denitrification of waste water

The experimental studies were concentrated on a down-flow denitrification filter and two biological approaches were tested.

4.2.1. Biomass fully active

Fig. 4 shows that, unlike the experimental results, the simulated nitrate levels run out too quickly in the filter (other simulations failed with lower values of the maximum specific growth rate). This is due to the exponential growth of the biomass (first order) which leads to faster filter clogging; even with a very low value for the initial amount of biomass (this is the case in the figures), it is impossible to simulate

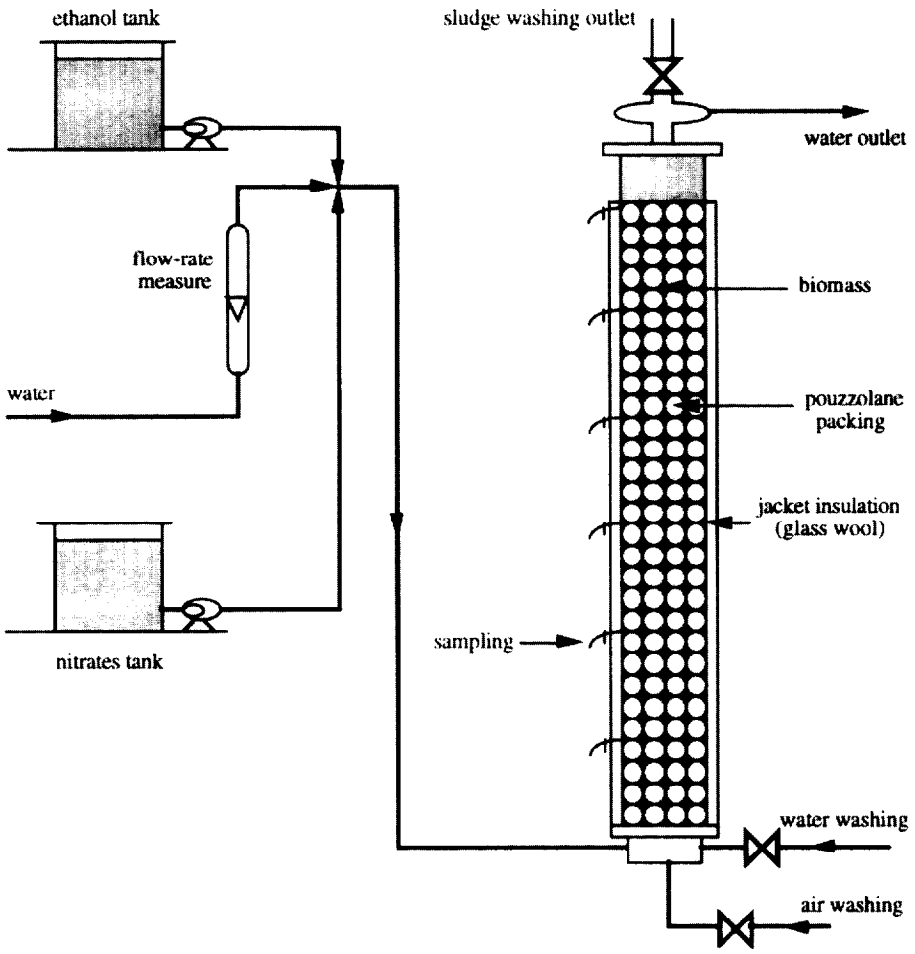

Fig. 3. Experimental pilot plant for drinking water denitrification.

the filter behaviour during all the treatment. Hence the kinetic model is not correct and the development the active/deactivated biomass concept was chosen

4.2.2. Active/deactivated concept

It is now possible to simulate biofilter behaviour during its whole lifetime. Good fits are obtained, with different liquid flow-rates, for the outlet concentration of suspended particles which instantaneously reaches a constant value (Figs. 5 and 6). Thus, the filtration part of the model may be validated.

As expected, a 'steady-state' is observed in Fig. 7 with constant outlet concentrations (the simulation is stopped with the state event detection: $\Delta P = \Delta P_{max}$) and the nitrates run out only in the second half of the filter (Fig. 8). Thus, from a qualitative point of view, good results are obtained for the biological part of the model. Unfortunately, these experimental denitrification results cannot be used for quantitative studies because they were obtained with waste water coming directly from a treatment plant with high uncontrolled variations in input concentrations. That is the reason why it has been decided to test the model for different applications on synthetic waters, with better control of input variables.

4.3. Application to the denitritation of a synthetic water

The experiments were achieved on a synthetic water (with sodium acetate as carbon source) which allows a constant feed concentration to be obtained. The use of a synthetic water enables separate study of the biological and filtration aspects and, in this case, for the validation of the biological model as the experiments were conducted without suspended particles.

Once again the filter (with liquid in down flow) was packed with a very porous material (pouzzolane) which retains a large amount of residual active microorganisms after washing. Thus, the biofilter reaches steady-state nearly instantaneously with constant outlet concentrations; this is why only figures with space concentration profiles are presented.

Good agreement was obtained between simulated and experimental data for concentrations of nitrites (Figs. 9 and 11) and carbon (Figs. 10 and 12), with different liquid flow-rates, during the whole treatment time. Thus, this approach appears much more realistic than the previous one and the biological part of the model may be validated.

4.4. Application to the denitrification of a synthetic drinking water

For drinking water treatment, very drastic constraints have to be observed concerning oxidized nitrogen ($[NO_2^-] + [NO_3^-] < 5.6$ mg N L^{-1}). Thus, both nitrite and nitrate concentrations have been measured; this is the reason they have

Table 3
Kinetic, stoichiometric and filtration parameter values used for different applications

	Denitrification of waste water	Denitritation	Denitrification of drinking water
Y_H (/(g DCO biomass g^{-1} DCO substrate))	0.67[a]	0.4[a]	0.3[a]
μ_H ($/j^{-1}$)	4[b]	5[c]	–
μ_1 ($/j^{-1}$)	–	–	5[c]
μ_2 ($/j^{-1}$)	–	–	7.5[c]
X_{Amax} (/(mg DCO L^{-1}))	1000[d]	480[d]	740[d]
K_S (/(mg CDO L^{-1}))	10[b]	40[c]	40[c]
K_{NO3} (/(mg N L^{-1}))	0.2[b]	5[c]	1[c]
K_{NO2} (/(mg N L^{-1}))	–	–	3[c]
k ($/m^{-1}$)	0.6[a]	–	–

[a] Experimental values.
[b] Values given with the IAWPRC model for waste water [5].
[c] Fixed values obtained by a synthesis of the appropriated literature.
[d] Values obtained by a quick trial/error strategy.

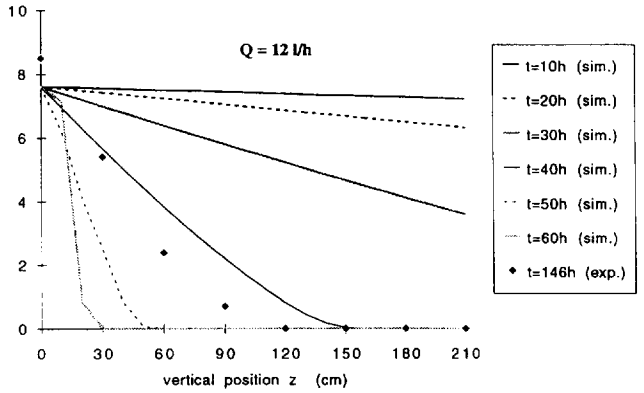

Fig. 4. Waste water denitrification: concentration profiles for nitrates in the filter (mg N-NO_3 L^{-1}).

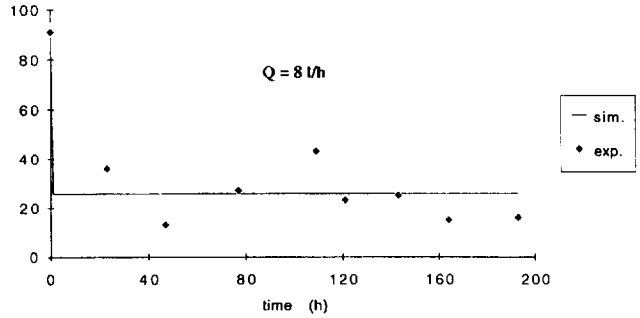

Fig. 5. Waste water denitrification: outlet concentration of suspended particles (mg L^{-1}).

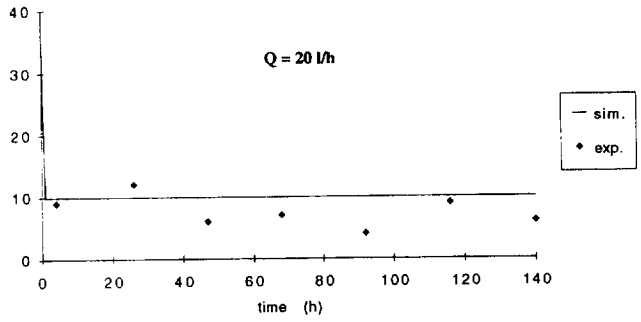

Fig. 6. Waste water denitrification: outlet concentration of suspended particles (mg L^{-1}).

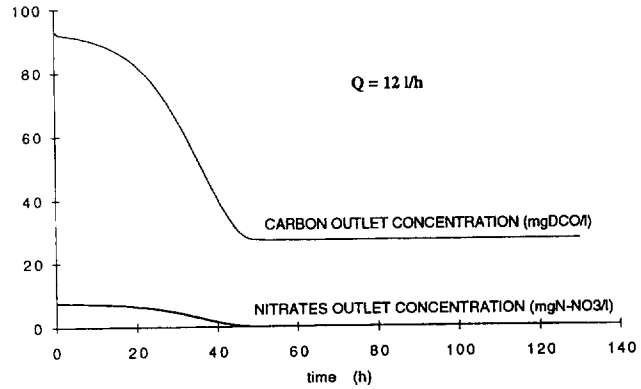

Fig. 7. Waste water denitrification (M_a/M_d): outlet concentrations of carbon and nitrate.

been dissociated in the model. The biological reaction ($NO_3^- \rightarrow N_2$) is represented schematically in two consecutive reactions, denitratation (1) and denitritation (2):

$$NO_3^- \xrightarrow{(1)} NO_2^- \xrightarrow{(2)} N_2$$

In terms of degrees of reduction, the denitratation reaction (1) may be written:

$$\frac{1}{Y_H}S + \frac{1-Y_H}{2.86Y_H}NO_3^- \rightarrow \text{biomass} + \frac{1-Y_H}{1.71Y_H}NO_2^-$$

with a corresponding growth rate:

$$r_1 = \mu_1 \eta_g \left(\frac{S_S}{S_S + K_S}\right)\left(\frac{S_{NO_3}}{S_{NO_3} + K_{NO_3}}\right)X_A$$

The denitritation reaction (2) is written as:

$$\frac{1}{Y_H}S + \frac{1-Y_H}{1.71Y_H}NO_2^- \rightarrow \text{biomass}$$

with

$$r_2 = \mu_2 \eta_g \left(\frac{S_S}{S_S + K_S}\right)\left(\frac{S_{NO_2}}{S_{NO_2} + K_{NO_2}}\right)X_A$$

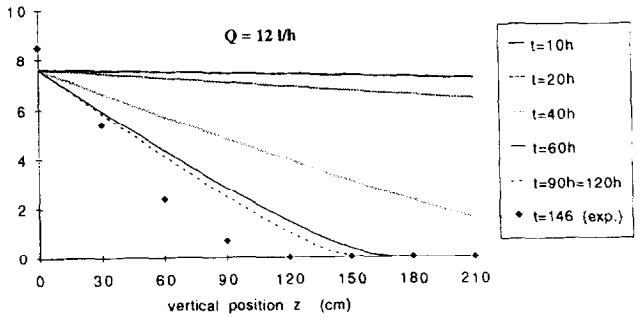

Fig. 8. Waste water denitrification (M_a/M_d): concentration profiles for nitrates in the filter (mg N-NO_3 L^{-1}).

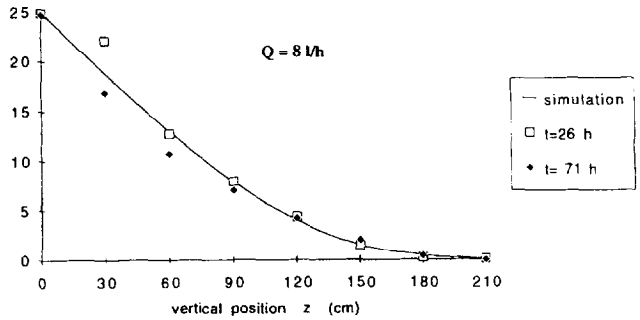

Fig. 9. Denitritation: concentration profiles for nitrites in the filter (mg N-NO_2 L^{-1}).

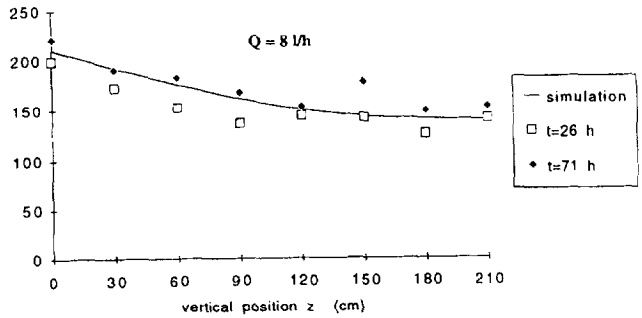

Fig. 10. Denitritation: concentration profiles for carbon in the filter (mg N-NO_2 L^{-1}).

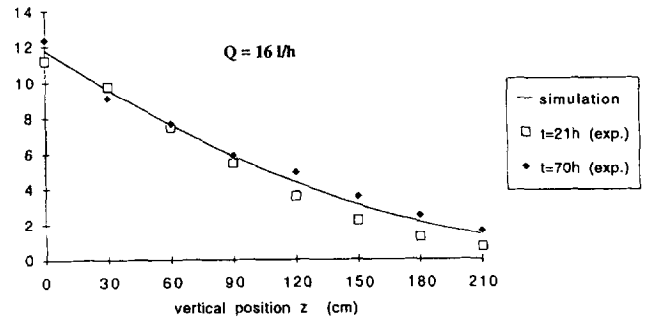

Fig. 11. Denitritation: concentration profiles for nitrites in the filter (mg DCO L^{-1}).

The same bacterial species work in the two reactions, in nearly the same environment, so we may assume that the two yields (Y_H) are equal.

The experiments were performed with synthetic water (using ethanol as the organic carbon source) in the upstream flow.

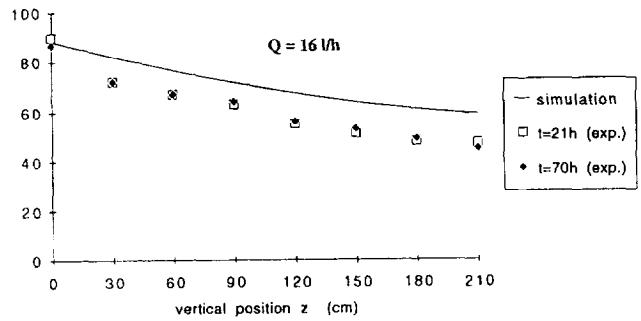

Fig. 12. Denitritation: concentration profiles for carbon in the filter (mg DCO L^{-1}).

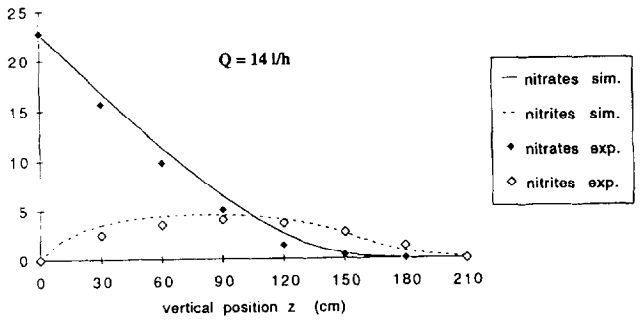

Fig. 13. Drinking water denitrification: concentrations profiles for nitrates and nitrites in the filter (mg N L^{-1}).

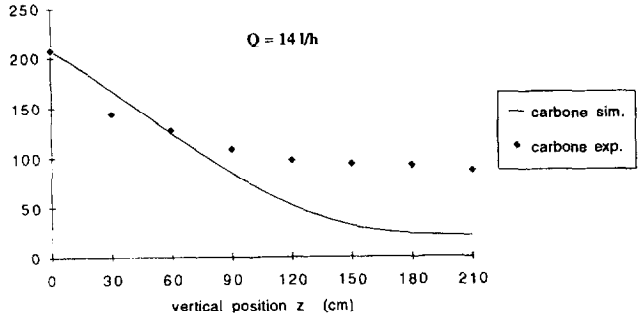

Fig. 14. Drinking water denitrification: concentration profiles for carbon in the filter (mg DCO L^{-1}).

Good agreement between experimental and simulated data were obtained for nitrate and nitrite levels (Fig. 13). The retention of nitrites in the filter can be observed as their concentration gets close to zero when there are no more nitrates.

The results for carbon are not as good (Fig. 14) but it must be noted that all these simulations were performed without real estimation of the kinetic and stoichiometric parameters. A better fit between experiments and simulations could be obtained by using a rigorous parameter estimation procedure for the determination of very sensitive parameters such as maximum growth rates or maximum active biomass concentrations in the filter.

5. Conclusion

A general model has been developed for the dynamic simulation of waste-water treatment units by submerged biofil-

ters. When used for carbon removal, denitrification or nitrification, this model allows for the investigation of the response of this type of unit to load and flow-rate perturbation. It will help designers to predict overall behaviour (removal efficiency and filter clogging) with control strategies in mind. The accuracy of the model and the efficiency of the implemented numerical method (even in hard integration conditions such as biofilter start-up) have been illustrated in the cases of denitritation and denitrification with comparison versus pilot plant data.

Further work needs to be performed especially in the evaluation of the pressure drop in the filter. The model should also be improved by taking into account the influence of temperature on the biological kinetics. The development of a specially adapted method for parameter estimation PDAE system, as well as the opportunity to introduce a moving grid in the method of lines should be investigated.

This work is dedicated to the memory of Professor B. Capdeville.

6. Nomenclature

d_{cell} cell density in the biofilm (g (COD) m^{-3})
d_{part} particle density in the particle deposit (g m^{-3})
$\boldsymbol{D}$ matrix of the coefficients associated with the dynamic terms $\partial \mathbf{s}/\partial t$ (–)
D_p packing particle diameter (m)
$\boldsymbol{J}$ jacobian matrix (–)
k filtration coefficient (m^{-1})
K_A electron acceptor half-saturation coefficient (g m^{-3})
K_D electron donor half-saturation coefficient g (COD) m^{-3}
$\boldsymbol{M}$ dynamic operator matrix (–)
n number of equations of the PDAE system (–)
N number of discretization points (–)
$\boldsymbol{p}$ vector of input variables (–)
Q liquid flow rate ($m^3\ h^{-1}$)
r reaction rate (biological or physical) (g $m^{-3}\ h^{-1}$)
$\boldsymbol{s}$ vector of state variables (–)
S_A electron acceptor concentration in liquid phase (g m^{-3})
S_D electron donor concentration in liquid phase (g (COD) m^{-3})
t time (h)
$\boldsymbol{u}$ vector of control variables (–)
U_m superficial velocity (m h^{-1})
X_A active biomass concentration in the filter (g (COD) m^{-3})
X_B total biomass concentration in the filter (g (COD) m^{-3})
X_D deactivated biomass concentration in the filter g (COD) m^{-3})
X_{Ml} suspended solid concentration in the liquid phase g m^{-3}
X_{Mr} retained particles concentration in the filter g m^{-3}
Y_H heterotrophic biomass yield (–)
z vertical position in the filter (m)
ΔP pressure drop in the filter (Pa)
ϵ porosity (–)
μ dynamic viscosity of the liquid (kg $m^{-1}\ s^{-1}$)
μ_o specific growth rate for biomass (h^{-1})
μ_{max} maximum specific growth rate for heterotrophic or autotrophic biomass (μ_H or μ_A) (h^{-1})
ν stoichiometric coefficient (–)
Ω cross-sectional area of the filter (m^2)
σ retention in the filter (–)

Acknowledgements

This work is part of J. Jacob's Ph.D. Thesis. We gratefully acknowledge the French Ministry of Research and Technology (MRT) and the Midi-Pyrénées Region (CCRRDT) for their financial support as well as the SAUR (BOUYGUES) Company for support of laboratory research.

References

[1] I. Farag, I. Gosling, R. Field and C.C. Chen, Simulating waste water treatment processes, *The Chemical Engineer*, (Sept. 1990) 31–38.
[2] G.G. Patry and I. Takacs, GPS-X: A waste water treatment plant simulator, *Proc. Mathmod Vienna (IMACS), Vienna, Austria, 1994*, pp. 456–459.
[3] M.N. Pons, O. Potier, N. Roche, F. Colin and C. Prost, Simulation of municipal waste water treatment plants by activated sludge, *Comp. Chem. Eng., 17 (suppl.)* (1993) 227–232.
[4] P. Lessard and B. Beck, Simulation dynamique d'une usine de traitement des eaux usées, *Tribune de l'eau, n° 533/5* (1991) 35–51.
[5] M. Henze, C.P. Leslie Grady, W. Guyer, G.V.R. Marais and T. Matsua (IAWPRC task group), A general model for single sludge waste water treatment systems, *Water Res., 21(5)* (1987) 505–515.
[6] P. Le Cloirec, G. Martin, B. Ben Barka and A.Y. Le Roux, Un modèle mathématique de la dénitrification sur filtres soufre-carbonate de calcium, *Chem. Eng. J., 31* (1985) 9–18.
[7] S.E. Jorgensen and M.J. Gromiec, Mathematical models in waste water treatment, in *Developments in Environmental Modeling*, Elsevier, Amsterdam, 1985, pp. 473–524.
[8] G.E. Speitel, K. Dovantzis and F.A. Di Giano, Mathematical modelling of biogeneration in G.A.C. column, *J. Environ. Eng., 113* (1987) 32–48.
[9] K.J. Williamson and P.L. Mc Carty, Verification studies of the biofilm model for bacterial substrate utilisation, *J. Water Pollut. Control Fed., 48* (1976) 281–296.
[10] K.M. N'Guyen, Description et modélisation des films biologiques aerobies, *Ph.D. Thesis*, INSAT (n° 96), France, 1989.
[11] R. Belkhadir, Etude fondamentale des biomasses fixées. Description et modélisation des biofilms biologiques anaerobies, *Ph.D. Thesis*, INSAT (n° 18), France, 1986.
[12] S. Elmaleh, H. Labaquere and R. Ben Aim, Biological filtration through a packed column, *Water Res., 12* (1978) 41–46.
[13] K.J. Ives and A. Gur, Recherche sur l'optimisation de la filtration, *Centre Belge d'Etude et de Documentation des Eaux, 333–334* (1971) 377–384.

[14] C.R. O'Melia and W. Ali, The role of retained particles in deep bed filtration, *Prog. Water Technol., 10* (1978) 167–182.
[15] J.P. Herzig and P. Le Goff, Le calcul prévisionnel de la filtration à travers un lit épais, *Chimie et Industrie Génie Chimique, 104* (1971) 2337–2346.
[16] R.B. Bird, *Transport Phenomena*, Wiley International Edition, 1960.
[17] W.E. Schiesser, *An Introduction to the Numerical Method of Lines Integration of Partial Differential Equations* (Differential Systems Simulator, Version 2), Lehigh Universities and Naval Air Development Center, 1977.
[18] C. Gear, The automatic integration of ordinary differential equations, *Commun. ACM, 14(3)* (1971) 176–179.
[19] A.C. Hindmarsh, LSODE and LSODI, two new initial value ordinary differential equation solvers, *ACM SIGNUM Newsletter, 15* (1980) 10–11.
[20] L. Petzold, DASSL: differential algebraic system solver, *Technical Report*, Sandia National Laboratories, Livermore, California, 1983.
[21] J. Albet, Simulation rigoureuse de colonnes de distillation discontinue à séquences opératoires multiples, *Ph.D. Thesis*, INP Toulouse, France, 1992.